

This discussion paper is/has been under review for the journal Geoscientific Model Development (GMD). Please refer to the corresponding final paper in GMD if available.

# An integrated Dissolved Organic Carbon Dynamics Model (DOCDM 1.0): model development and a case study in the Alaskan Yukon River Basin

X. Lu<sup>1,a</sup> and Q. Zhuang<sup>1,2</sup>

<sup>1</sup>Department of Earth, Atmospheric, Planetary Sciences, Purdue University, West Lafayette IN, 47907, USA

<sup>2</sup>Department of Agronomy, Purdue University, West Lafayette, 47907, USA

<sup>a</sup>now at: The Ecosystems Center, the Marine Biological Laboratory, Woods Hole, MA, 02536, USA

Received: 28 September 2015 – Accepted: 8 November 2015 – Published: 10 December 2015

Correspondence to: Q. Zhuang (qzhuang@purdue.edu)

Published by Copernicus Publications on behalf of the European Geosciences Union.

Title Page

Abstract

Introduction

Conclusions

References

Tables

Figures

⏪

⏩

◀

▶

Back

Close

Full Screen / Esc

Printer-friendly Version

Interactive Discussion



## Abstract

Quantitative understanding of the variation in dissolved organic carbon (DOC) is important to studying the terrestrial ecosystem carbon cycle. This study presents a process-based, dissolved organic carbon dynamics model (DOCDM 1.0) that couples the soil heat conduction, water flow, DOC production, mineralization and transport in both surface and subsurface of soil profile to quantify DOC dynamics in boreal terrestrial ecosystems. The model is first evaluated and then applied for a watershed in Alaska to investigate its DOC production and transport. We find that 42 and 27 % of precipitation infiltrates to soils in 2004, a warmer year, and in 1976, a colder year, respectively. Under warming conditions, DOC transported via overland flow does not show the expected decrease trend while the overland DOC yield shows a 4% increase. The horizontal subsurface flow only accounts for 1–2 % of total water flux, but transports 30–50 % of DOC into rivers. Water flush due to water infiltration controls DOC transport. Snowmelt plays a noticeable role in DOC flush-out and DOC transport significantly depends on flowpaths in the study region. High soil temperature stimulates DOC production. The overland DOC export does not necessarily follow the DOC downward trend in surface water transport. Overall, this study shows that DOC export behavior is complex under changing temperature and hydrological conditions in cold-region watersheds. To adequately quantify DOC dynamics in northern high latitudes, more DOC and hydrological data are needed to better parameterize and test the developed model before extrapolating it to the region.

## 1 Introduction

Dynamics of dissolved organic carbon (DOC) are a critical, yet often neglected component of the terrestrial carbon cycle. The significance of DOC has been stressed by previous studies in many aspects, including its influence on nutrient cycling (Qualls and Haines, 1991; Michalzik and Matzner, 1999), its service as a microbial energy source

GMDD

8, 10411–10454, 2015

### An integrated Dissolved Organic Carbon Dynamics Model (DOCDM 1.0)

X. Lu and Q. Zhuang

Title Page

Abstract

Introduction

Conclusions

References

Tables

Figures



Back

Close

Full Screen / Esc

Printer-friendly Version

Interactive Discussion



## An integrated Dissolved Organic Carbon Dynamics Model (DOCDM 1.0)

X. Lu and Q. Zhuang

Title Page

Abstract

Introduction

Conclusions

References

Tables

Figures



Back

Close

Full Screen / Esc

Printer-friendly Version

Interactive Discussion



(Baker et al., 2000; Raymond and Bauer, 2000) and its effects on pollutant transport (Morris and Hargreaves, 1997). High latitude ecosystems, which store about one-third of the global terrestrial organic carbon (Gorham, 1991; Moore, 2002), play a vital role in determining the future terrestrial carbon cycle including DOC dynamics, under rapidly changing climatic conditions. Dramatic changes have occurred in the arctic cryosphere, biosphere, and atmosphere (Hinzman et al., 2005; Serreze et al., 2000), resulting in higher DOC concentrations in the Arctic rivers in comparison with other major river basins on the globe (Lobbess et al., 2000; Raymond et al., 2007), and the DOC flux is expected to increase in the future (Freeman et al., 2001; Tranvik and Jansson, 2002).

While the important role of DOC in regulating C transport from terrestrial ecosystems to river systems is acknowledged, the production, loss, stabilization and release of DOC, and the interaction of these processes with external environmental variables, are still not well understood. Sorption and desorption processes are widely believed to be the dominant controlling mechanisms for DOC transport through solid soil matrices (Quails and Haines, 1992a, b). Soluble DOC may be lost in sorption process or as a result of microbial mineralization, and DOC sorbed to the soil column may rejoin water during desorption process or transformed into CO<sub>2</sub> via degradation. At a drainage basin scale, more hydrological, land cover, catchment characteristics and soil thermal factors should also be considered in quantifying DOC patterns in stream flow. The location and distribution of flow pathways and residence times of water are among those controls to be considered. When watersheds are in low-flow periods, predominant subsurface flows usually have low DOC concentrations presumably due to their relatively deep flowpaths in mineral layers. Rainfall and snowmelt events shift DOC transport from subsurface to surface-water system. Rising water table and increasing flow flush the DOC-rich superficial soil water to the stream channels (Hornberger et al., 1994; Dutta et al., 2006).

The DOC export from northern high latitude ecosystems has more variations due to spring snowmelt, increasing temperature, and associated permafrost thawing (Ågren et al., 2010). A large portion of the annual DOC delivery into high northern latitude



step. It provides ground surface temperature, throughfall and snowmelt rates, which are needed in the soil heat conduction and water infiltration modules. The soil heat and water infiltration module then estimates the soil temperature profile, soil ice content and water infiltration rate by solving soil thermal and moisture equations. Finally, the DOC production, sorption and desorption, mineralization and transport processes are modeled in the DOC dynamic module. Below we describe each module (also see the detailed information in Supplement A).

## 2.1 Vegetation and land surface process module

The land surface process module (Fig. 1) integrates hydrological and energy processes to simulate overland and channel flow dynamics, which drive the DOC horizontal transport. Precipitation is partitioned to rain and snow according to air temperature. Canopy layer interception is a function of leaf area index (Dickinson et al., 1986). Snow accumulation and melt are simulated when there is snow on the ground and snowfall. Snowpack is treated as a two-layer medium, and its accumulation and ablation is estimated by solving mass and energy balance equations (Andreadis et al., 2009). The energy exchange on the snowpack is modeled based on the net radiation, sensible heat carried by convection, heat advected by rainfall, evaporation, sublimation, condensation and latent heat loss or gain due to melting and refreezing. Processes such as snow accumulation and ablation, dynamics in the snow water equivalent, and meltwater yield are represented in the mass balance equation. In the snow model, snow interception (Storck et al., 2002), atmospheric stability (Anderson, 1976; Tarboton et al., 1995) and blowing snow (Bowling et al., 2004) processes are considered. Total evapotranspiration is based on the Penman–Monteith equation (Monteith, 1990) and has three components: (1) evaporation from bare soil, (2) evaporation from canopy and (3) transpiration from canopy. The vegetation module (green section of Fig. 1) provides radiation and wind speed attenuation, architectural and stomatal resistance, and roughness length to estimate snow and rain interception, evapotranspiration and root uptakes. It also provides the vegetation type information required in the DOC production estimation. The

### An integrated Dissolved Organic Carbon Dynamics Model (DOCDM 1.0)

X. Lu and Q. Zhuang

Title Page

Abstract

Introduction

Conclusions

References

Tables

Figures



Back

Close

Full Screen / Esc

Printer-friendly Version

Interactive Discussion



equations within the two modules are adopted from a large-scale hydrology model, the variable infiltration capacity (VIC) model (Liang et al., 1994).

Rainfall could contribute to surface or subsurface hydrological systems through infiltration, which controls the pathway of DOC transport. In arctic regions, the soil ice directly affects infiltration and heat conduction within the soil profile (Cherkauer and Lettenmaier, 1999, 2003; Cherkauer et al., 2003).

## 2.2 Soil heat conduction and water infiltration module

In cold regions, soil heat conduction is affected by liquid water and ice distribution; on the other hand, infiltration and water movement in soils is also influenced by changes of ice content. In this module, heat conduction and vertical water movement are resolved at a 90 s time step. When infiltration occurs, the time step is adjusted to 1 s (red section of Fig. 1). Here we made several assumptions: (1) ice is immovable and only liquid water can move in frozen soils, (2) the influences of vapor transport on water and heat conduction can be ignored, (3) liquid flows due to thermal gradients and heat conduction by convection can be neglected; and (4) unfrozen water and the subzero temperatures of frozen soils are included in the dynamic equilibrium. Under these assumptions, water movement and heat conduction only occurs in the vertical direction and can be described with one-dimensional equations.

### 2.2.1 Vadose zone modeling

The one-dimensional Richards equation (Richards, 1931) is used to describe vertical water movement in both frozen and unfrozen soils:

$$\frac{\partial \theta_L(h)}{\partial t} + \frac{\rho_i}{\rho_L} \cdot \frac{\partial \theta_i(T)}{\partial t} = \frac{\partial}{\partial z} \left[ K(h) \cdot \frac{\partial h}{\partial z} + K(h) \right] + S \quad (1)$$

Where  $\theta_L$  is volume liquid water content ( $L^3 L^{-3}$ ),  $\theta_i$  is volume ice content ( $L^3 L^{-3}$ ),  $t$  is time (T),  $K$  is hydraulic conductivity ( $L T^{-1}$ ),  $z$  is the spatial coordinate positive

downward,  $\rho_i$  is the density of ice ( $\text{ML}^{-3}$ ) ( $931 \text{ kg m}^{-3}$ ),  $\rho_L$  is the density of liquid water ( $\text{ML}^{-3}$ ) ( $1000 \text{ kg m}^{-3}$ ),  $h$  is the capillary-pressure head (L),  $T$  is the temperature (K), and  $S$  is a sink/source term ( $T^{-1}$ ) due to groundwater movement (Sect. 2.4.2).

By defining:

$$\theta = \theta_L + \frac{\rho_i}{\rho_L} \cdot \theta_i \quad (2a)$$

We have:

$$\frac{\partial \theta}{\partial t} = \frac{\partial}{\partial z} \left[ K(h) \cdot \frac{\partial h}{\partial z} + K(h) \right] + S \quad (2b)$$

Equation (2b) is numerically solved (Supplement B) by using fully implicit approximation and the discretization form proposed by Celia et al. (1990). The constant head could be used as the upper boundary condition for Eq. (1) when overland exists; the amount of rainfall during no overland condition decided whether constant flux or no flux should be used. Free drainage ( $\text{Flux}_{\text{bottom}} = K_{\text{bottom}}$ ) and no flux ( $\text{Flux}_{\text{bottom}} = 0$ ) are the two common options for setting the lower boundary condition. We found the free drainage resulted in too much leakage and no-flux bottom, on the other hand, produced too much moisture in soil. Here we set the bottom flux is determined by  $\text{Flux}_{\text{bottom}} = \varepsilon \cdot K_{\text{bottom}}$  where  $0 \leq \varepsilon \leq 1$ . In northern high latitudes,  $\varepsilon$  may increase due to permafrost degradation (Lu and Zhuang, 2011). By comparing the simulated annual flow to the measurements, we set  $\varepsilon$  as 0.21 and 0.43 for the simulations of 1976 and 2004, respectively. See the Supplement B for the detailed derivation and boundary conditions setting. The relationships between  $\left(\frac{d\theta}{dh}\right)$ ,  $h$ , and  $K$  are proposed by van Genuchten (1980):

$$\begin{cases} \theta(h) = \frac{(\theta_s - \theta_r)}{(1 + (a|h|)^{n'})^{m'}} + \theta_r \\ K(h) = K_s \frac{\left\{ \left(1 - (a|h|)^{n'-1}\right) \left(1 + (a|h|)^{n'}\right)^{-m'} \right\}^2}{(1 + (a|h|)^{n'})^{m'/2}} \end{cases} \quad (3)$$

Where  $\theta_s$ ,  $\theta_r$  and  $K_s$  are saturated water content ( $L^3 L^{-3}$ ), residual water content ( $L^3 L^{-3}$ ) and saturated hydraulic conductivity ( $LT^{-1}$ ), respectively;  $a$ ,  $m'$  and  $n'$  are model parameters, and are set as 0.0335, 0.5 and 2, respectively.

The presence of ice may significantly reduce water flow in the porous medium. The scheme of Hansson et al. (2004) is used to address the ice effect. The hydraulic conductivity for the liquid water portion of the partially frozen soil,  $K_f$  is defined as:

$$K_f(h) = 10^{-\varphi Q} \cdot K(h) \quad (4)$$

Where  $\varphi$  is the impedance factor (Lundin, 1990) and  $Q$  is the ratio of ice content to the total (minus the residual) water content.  $\varphi$  is assumed to be 7.

## 2.2.2 Soil heat transfer

The heat transfer in soils is modeled as:

$$\frac{\partial(C' \cdot T)}{\partial t} - L_f \cdot \rho_i \frac{\partial \theta_i}{\partial t} = \frac{\partial}{\partial z} \left( \lambda \frac{\partial T}{\partial z} \right) \quad (5)$$

where  $T$  is the soil temperature ( $^{\circ}C$ ) and the volumetric heat capacity of the soil,  $C'$  ( $Jm^{-3}K^{-1}$ ) is defined as the weighted volumetric heat capacity of the soil ( $C'_s$ ), liquid water ( $C'_L$ ) and ice ( $C'_I$ ) phases, multiplied by their respective volumetric fractions:

$$C' = C'_s \theta_s + C'_w \theta_L + C'_I \theta_I \quad (6)$$

and  $L_f$  is the volumetric latent heat of freezing ( $Jkg^{-1}$ ) (approximately  $3.34 \times 10^5$ ).  $\rho_i$  and  $\theta_i$  are ice density and content, respectively.  $\lambda$  is soil thermal conductivity

Title Page

Abstract

Introduction

Conclusions

References

Tables

Figures

◀

▶

◀

▶

Back

Close

Full Screen / Esc

Printer-friendly Version

Interactive Discussion



( $W m^{-1} K^{-1}$ ). Thermal conductivity is calculated with the method in Johansen (1975):

$$\lambda = (\lambda_{\text{sat}} - \lambda_{\text{dry}}) \cdot \lambda_e \quad (7a)$$

$$\lambda_{\text{sat}} = \begin{cases} 0.5^n \cdot (7.7^q 2.0^{1-q})^{1-n''} & \text{unfrozen} \\ 0.5^n \cdot (7.7^q 2.0^{1-q})^{1-n''} \cdot 0.269^{W_u} & \text{frozen} \end{cases} \quad (7b)$$

$$\lambda_{\text{dry}} = \frac{0.17 \cdot \gamma_d + 64.7}{2700 - 0.947 \cdot \gamma_d} \quad (7c)$$

$$\lambda_e = \begin{cases} \log S_r + 1 & \text{unfrozen} \\ S_r & \text{frozen} \end{cases} \quad (7d)$$

Where  $n''$  is the porosity,  $q$  is the quartz content,  $W_u$  is the fractional volume of unfrozen water,  $\gamma_d$  is bulk density ( $kg m^{-3}$ ) and  $S_r$  is the fraction degree of saturation. In the above soil thermal equation, the convection of sensible heat with flowing water and uptake energy associated with root water uptake are not considered. The fraction of unfrozen water is needed in order to estimate heat capacity  $C'$  and soil thermal conductivity  $\lambda$ . The formula proposed by Flerchinger and Saxton (1989) is used:

$$W = W^C \left( \left( \frac{1}{g \varphi_e} \right) \cdot \left( \frac{L_f \cdot T}{T + 273.16} \right) \right)^{-B_p} \quad (8)$$

Where  $W$  is the liquid water content,  $W^C$  is the maximum water content,  $g$  is acceleration due to gravity,  $\varphi_e$  is the air entry potential and  $B_p$  is the pore-size distribution.

# GMDD

8, 10411–10454, 2015

## An integrated Dissolved Organic Carbon Dynamics Model (DOCDM 1.0)

X. Lu and Q. Zhuang

Title Page	
Abstract	Introduction
Conclusions	References
Tables	Figures
◀	▶
◀	▶
Back	Close
Full Screen / Esc	
Printer-friendly Version	
Interactive Discussion	



Similarly, the fully implicit discretization form (Hansson et al., 2004) for Eq. (5) is:

$$C_i^{n+1,m} \cdot \frac{T_i^{n+1,m+1} - T_i^n}{\Delta t} - \left[ L_f \cdot \rho_l \cdot \left( \frac{d\theta_l}{dT} \right)_i^{n+1,m} \cdot \frac{T_i^{n+1,m+1} - T_i^{n+1,m}}{\Delta t} \right] - L_f \cdot \rho_l \frac{(\theta_l)_i^{n+1,m} - (\theta_l)_i^n}{\Delta t} = \frac{\lambda_{i+1/2}^{n+1,m} \cdot \left( \frac{T_{i+1}^{n+1,m+1} - T_i^{n+1,m+1}}{\Delta z} \right) - \lambda_{i-1/2}^{n+1,m} \cdot \left( \frac{T_i^{n+1,m+1} - T_{i-1}^{n+1,m+1}}{\Delta z} \right)}{\Delta z} \quad (9)$$

Where  $i$ ,  $\Delta z$  and  $T^n$  denote the spatial location, node size and the approximate value of  $T$  at the  $n$ th discrete time level, respectively,  $\Delta t \equiv t^{n+1} - t^n$  is the time step.  $\frac{d\theta_l}{dT}$  is evaluated by Eq. (8). Because of the dependency of the apparent volumetric heat capacity ( $C'$ ) and thermal conductivity ( $\lambda$ ) on temperature, Eq. (9) is also highly nonlinear. The same iteration scheme used for the above Richards equation is also used to linearize the two nonlinear items, and  $m$  stands for iteration level. In Eq. (9), the subscripts  $i - 1/2$  and  $i + 1/2$  represent the upper and lower grid interfaces, respectively. Hydraulic conductivity and soil thermal conductivity at grid interface is calculated using geometric averaging. Equations (1) and (5) are coupled due to their mutual dependence on water content, pressure heads and temperature. The lower boundary for Eq. (9) is set to zero thermal flux. The upper boundary condition is set to the soil surface temperature (it is iteratively solved by closing the surface energy balance) or snowpack temperature if snow exists. Supplement B lists the steps for setting these two types of boundary conditions.

### 2.3 DOC module

A typical convection-dispersion equation is used to characterize the DOC transport (Patankar, 1980). Three processes are considered in the DOC transport: (1) one-dimensional infiltration, (2) two-dimensional overland transport; and (3) two-dimensional saturated subsurface flow transport (Fig. 1). Since most of current DOC measurements

## An integrated Dissolved Organic Carbon Dynamics Model (DOCDM 1.0)

X. Lu and Q. Zhuang

Title Page

Abstract

Introduction

Conclusions

References

Tables

Figures

◀

▶

◀

▶

Back

Close

Full Screen / Esc

Printer-friendly Version

Interactive Discussion



were acquired for very large regions, it is difficult to get the DOC-related parameters for typical land cover types. In this study, we used the available data from previous studies to derive type-specific parameters for those types having no direct measurements (Supplement C). The DOC desorption and microbial production processes are treated as DOC sources, and sorption and mineralization processes are sink terms. Point processes including DOC production, mineralization, sorption and desorption processes as well as DOC infiltration and two-dimensional DOC transport processes are detailed below.

### 2.3.1 DOC production, mineralization, sorption and desorption

The equations in Yurova et al. (2008) are used to estimate the DOC production rate ( $\text{mg g}^{-1} \text{h}^{-1}$ ):

$$P = P_{\text{basal}} \cdot Q_{10}^{(T - T_{\text{basal}})/10} \quad (10)$$

$$P_{\text{anp}} = P \cdot K_{\text{anp}} \quad (11)$$

Where  $Q_{10}$  is the increase in metabolic rates per  $10^\circ\text{C}$  increase in soil temperature (Table 1), and  $T_{\text{basal}}$  is the reference temperature ( $20^\circ\text{C}$  in this study) when basal rates of DOC production  $P_{\text{basal}}$  ( $\text{mg g}^{-1} \text{h}^{-1}$ ) are measured (Table 1). The fraction  $K_{\text{anp}}$  (Table 1) is used to correct the anoxic rates of DOC production on the corresponding DOC production rate ( $P_{\text{anp}}$ ) under aerobic conditions. Since DOC production is highly related to the soil organic carbon pool, we use plant rooting depth to approximate soil organic carbon distribution. The DOC production rate reduces 95 % ( $0.05 \cdot P_{\text{basal}}$ ) at the depth which is not located in the organic layer.

Sorption and desorption are two key mechanisms regulating DOC stabilization and release rates. Here soluble organic carbon includes dissolved (DOC) and potentially soluble, but currently solid (PDOC). PDOC can exist as suspended particulates or in soil surface and sediment. The total concentration of DOC ( $C_T''''$ ;  $\text{g cm}^{-3}$ ) can be calcu-



$T_{\text{basal}}$  is the reference rate (20 °C in this study) when basal rates of  $M_{\text{basal}}$  ( $\text{h}^{-1}$ ) (Table 1) are measured. Also, the microbial mineralization rate of PDOC is assumed to be only 1/6 ( $K$ , Table 1) of the normal decomposition rate. Soil temperature used in the DOC production and mineralization is acquired by solving the soil heat transport equation (Sect. 2.2.2). These DOC processes are illustrated in Fig. 2.

### 2.3.2 DOC vertical movement

The vertical transport of DOC is modeled with the one-dimensional convection-dispersion equation:

$$\frac{\partial (\theta_I C_I''' + \theta_L C_L''')}{\partial t} = - \frac{\partial (q C''')}{\partial z} + \frac{\partial (\theta_L D \frac{\partial C'''}{\partial z})}{\partial z} + P' + M' + S' + R' \quad (15a)$$

$$D = D_{\text{dif}} + \lambda' \cdot \left| \frac{q}{\theta} \right| \quad (15b)$$

Where  $\theta_I$  and  $\theta_L$  are ice and liquid water content, respectively.  $t$  is the time (h),  $z$  is the soil depth (cm),  $C'''$  is the DOC concentration ( $\text{g mL}^{-1}$ ),  $q$  is the vertical water flux density ( $\text{cm h}^{-1}$ ), and  $D$  is the dispersion coefficient ( $\text{cm}^2 \text{h}^{-1}$ ).  $C_I'''$  is the DOC “concentration” in ice ( $\text{g mL}^{-1}$ ).  $D_{\text{dif}}$  and  $\lambda'$  are the molecular diffusion coefficient ( $\text{cm}^2 \text{h}^{-1}$ ) and dispersivity (cm), respectively (Table 1).  $P'$ ,  $M'$  and  $S'$  describe DOC production, mineralization and sorption/desorption ( $\text{g cm}^{-3} \text{h}^{-1}$ ) (Sect. 2.3.1 and Supplement D).  $R'$  is the DOC transfer rate from soil surface to overland flow (Sect. 2.4.3). By comparing Eq. (15) with Eq. (12), one may notice that we have assumed only DOC ( $\theta_L C'''$ ) can move in soil and PDOC ( $\rho_b S$ ) is attached on soil. In order to solve Eq. (15), it is necessary to know  $\theta_I$ ,  $\theta_L$  and  $q$  which are obtained from solutions to the soil thermal and the Richards equations (Sect. 2.2). The boundary conditions for Eq. (15) are the specified fluxes, which are equal to the water flux times the DOC concentrations. Since DOC vertical movement normally occurs with spring floods when convective flow dominates infiltration, the overland DOC concentration can be used as the DOC concentration at

Title Page

Abstract

Introduction

Conclusions

References

Tables

Figures

⏪

⏩

◀

▶

Back

Close

Full Screen / Esc

Printer-friendly Version

Interactive Discussion





Where  $h'$  is the surface flow depth (L),  $t$  is time,  $q_x$  and  $q_y$  are the unit flow rate in the  $x$  direction and  $y$  direction ( $L^2 T^{-1}$ ), respectively.  $e$  is the total throughfall and snow melt rate ( $L T^{-1}$ ), and  $S_{f_{x,y}}$   $S_{o_{x,y}}$  are friction and bed slopes (unitless) in the  $x$  and  $y$  direction, respectively.  $h'$  is calculated in the infiltration module (Sect. 2.2.1). The flow resistance must be determined by solving overland flow equations. Assuming that flow is turbulent and the Manning formulation (in S.I. units) can describe the resistance:

$$q_{x,y} = a_{x,y} h'^{\beta} \quad (18a)$$

The Manning approximations for  $a_{x,y}$  and  $\beta$  are:

$$a_{x,y} = \frac{S_{f_{x,y}}^{1/2}}{n} \quad (18b)$$

$$\beta = \frac{5}{3} \quad (18c)$$

Where  $n$  is the Manning's overland roughness coefficient, which can be estimated from the land-use map (Woolhiser, 1975).

The channel flow routing process is modeled with one-dimensional diffusive channel flow equation (Julien and Saghafian, 1991), which is derived in a similar manner to its two-dimensional overland counterpart with the exception that channel flow routing only happens in a finite space established for a given channel section. The one-dimensional continuity relationship can be expressed with the following equation:

$$\frac{\partial A}{\partial t} + \frac{\partial Q}{\partial X} = q_{in} - q_{out} \quad (19)$$

Where  $A$  is the channel flow cross-section area ( $L^2$ );  $Q$  is channel discharge ( $L^3 T^{-1}$ );  $q_{in}$  and  $q_{out}$  are lateral inflow and outflow per unit length ( $L^2 T^{-1}$ ), respectively. Furthermore, the flow within the channel is also assumed completely turbulent, and the

## GMDD

8, 10411–10454, 2015

### An integrated Dissolved Organic Carbon Dynamics Model (DOCDM 1.0)

X. Lu and Q. Zhuang

Title Page

Abstract

Introduction

Conclusions

References

Tables

Figures

◀

▶

◀

▶

Back

Close

Full Screen / Esc

Printer-friendly Version

Interactive Discussion



Manning's equation is used to estimate the channel discharge at a given time step:

$$Q = \frac{1}{n} AR^{\frac{2}{3}} s_f^{\frac{1}{2}} \quad (20)$$

Where  $R$  is the hydraulic radius (L);  $s_f$  is the friction slope (unitless) and  $n$  is the Manning roughness coefficient, respectively. Supplement E details the channel network building.

## 2.4.2 Saturated subsurface flow

The quasi- three-dimensional saturated subsurface flow model was used in this study. Each simulation cell can exchange water with its four adjacent neighbors. Local hydraulic gradients are approximated by local surface slopes. Therefore, a given grid will receive water from its upslope neighbors and discharge to its downslope neighbors. The subsurface routing method was not used for cells that contain perched water tables.

Under non-isothermal conditions, the effect of the ice layer on the subsurface flow should be considered. We used the soil profile of the two neighboring cells in order to illustrate our method (Fig. 3). The left column has one saturated zone whose thickness is  $H1$ , and its adjacent pixels shown in the right column may have four possible zones within the location of  $H1$ : top unsaturated layer ( $Z1$ ), frozen saturated layer ( $Z2$ ), liquid saturated layer ( $Z3$ ) and bottom ice layer ( $Z4$ ). One can deduce some relationships:  $0 \leq Z1 < H1$ ,  $0 \leq Z2 < H1$ ,  $0 \leq Z3 < H1$ ,  $0 \leq Z4 < H1$ ,  $Z1 + Z2 + Z3 + Z4 = H1$ .

The rate ( $L^3 T^{-1}$ ) of saturated subsurface flow from a specific cell to its down-gradient neighbors is modeled as:

$$Q_{i,j,d} = K_{i,j} \cdot D \cdot W' \cdot s \quad (21)$$

Where  $i, j$  are cell location indexes;  $d$  numbered from 0 to 7 represents directions between a cell and its eight adjacent eight neighbors;  $Q_{i,j,d}$  is the flow rate ( $L^3/T$ ) from

Title Page

Abstract

Introduction

Conclusions

References

Tables

Figures

⏪

⏩

◀

▶

Back

Close

Full Screen / Esc

Printer-friendly Version

Interactive Discussion



cell  $i, j$  in the  $d$  direction and  $W'$  is the width of flow in the  $d$  direction (L);  $K_{i,j}$  ( $LT^{-1}$ ) is the transmissivity at cell  $i, j$ ;  $s$  is the slope gradient in the  $d$  direction and  $D$  is the aquifer thickness (L).  $D$  is estimated according to the location of the unsaturated zones in the neighbor cells, as well as the phase of the saturated layer under the unsaturated zone. Specifically, for the left soil column in scenario A in Fig. 3, its neighbor cell has one ice layer (Z2) under the unsaturated zone (Z1). In this case, the aquifer ( $D$ ) has its lower boundary at the top of Z2. In the scenario B, there is no Z2 layer. Thus, the lower boundary of the aquifer ( $D$ ) is located at the top of the bottom ice layer (Z4). If there is no Z3 layer, the situation is similar to scenario A. Finally, the aquifer thickness is the same as H1 if there is no Z2, Z3, Z4 at all.

### 2.4.3 Two-dimensional DOC transport

In the overland transport, DOC might be transported with the flow to a certain distance from its production sites but then re-accumulate at this new point if overland flow is not persistent enough for the DOC to reach a river channel. In surface overland DOC transport, we only consider the advection process. For two-dimensional flow in the overland plane, a continuity (conservation of mass) equation can be written as:

$$\frac{\partial(\rho_b S + \theta_L C''_{ov})}{\partial t} = \frac{\partial(\mathbf{q}'_x \cdot C''_{TOV})}{\partial x} + \frac{\partial(\mathbf{q}'_y \cdot C''_{TOV})}{\partial y} + P' - M' + R' \quad (22)$$

Where  $C''_{TOV}$  is the total DOC (DOC and PDOC) concentration in overland flow ( $g mL^{-1}$ ),  $C''_{ov}$  is the DOC concentration in overland flow ( $g mL^{-1}$ ),  $t$  is the time, vector  $\mathbf{q}$   $\{\mathbf{q}_x, \mathbf{q}_y\}$  is composed of overland flow flux density in the  $x$  and  $y$  direction ( $cm s^{-1}$ ),  $P'$  and  $M'$  are the microbial DOC production and mineralization rates ( $g mL^{-1} s^{-1}$ ), respectively (Sect. 2.3.1). Similarly, Eq. (22) is still applicable for DOC transport in channels except that its one-dimensional version is used. In overland DOC transport, we assumed both DOC ( $\theta C$ ) and PDOC ( $\rho_b S$ ) are carried with water. For overland water, the soil bulk density ( $\rho_b$ ) is determined by the sediment concentration. In this study, we use

Title Page

Abstract

Introduction

Conclusions

References

Tables

Figures

◀

▶

◀

▶

Back

Close

Full Screen / Esc

Printer-friendly Version

Interactive Discussion



sediment concentration measured at the USGS gage station (USGS 15476000) to estimate the soil bulk density in overland flows (Supplement E). The DOC in soils may be transferred to surface runoff water ( $R'$ ), especially during periods of heavy rainfall or snowmelt. The mass coefficient is related to a variety of hydrological factors including rain intensity and duration, slope and soils:

$$R' = k' [c'''(0) - C'''_{ov}] / \Delta z \quad (23)$$

Where  $k'$  is the transfer coefficient ( $\text{cm s}^{-1}$ ) and  $c'''(0)$  is the DOC concentration at the soil surface. Equation (23) describes the rate-limited DOC transfer from the soil solution to the overland flow which is driven by the concentration gradient across the film layer that separates the stagnant soil solution and the moving overland flow (Wallach et al., 1988, 1989). The depth of the mixing zone ( $\Delta z$ ) is normally very small (Zhang et al., 1997) and it is assumed to be 2 cm in this study. By assuming that overland flow is turbulent, we follow the method proposed by Wallach et al. (1989) to estimate  $k'$ :

$$k' = \frac{D' \cdot n \cdot h'^{\frac{1}{3}} \cdot J^{\frac{1}{2}} \cdot \rho_L \cdot g}{\mu} \quad (24)$$

Where  $D'$  is the liquid diffusivity for DOC,  $n$  is the Manning roughness coefficient,  $h'$  is the overland water depth,  $J$  is the slope (fraction),  $\rho_L$  is the water density,  $g$  is the gravitational acceleration and  $\mu$  is the viscosity coefficient.

The DOC transport in the subsurface system is assumed to only occur with ground water movement, and the dispersion effect, explained below, is not considered:

$$\frac{\partial (\theta_L C''')}{\partial t} = (-Q_{sx} \cdot C''' - Q_{sy} \cdot C''') / V \quad (25)$$

Where  $Q_{sx}, Q_{sy}$  are the saturated subsurface flow in the  $x$  and  $y$  directions ( $\text{L}^3 \text{T}^{-1}$ ), respectively, estimated using the Darcy's law.  $V$  is the volume of one single simulation grid ( $\text{L}^3$ ). The subsurface DOC production, mineralization and sorption/desorption

## GMDD

8, 10411–10454, 2015

### An integrated Dissolved Organic Carbon Dynamics Model (DOCDM 1.0)

X. Lu and Q. Zhuang

Title Page

Abstract

Introduction

Conclusions

References

Tables

Figures

◀

▶

◀

▶

Back

Close

Full Screen / Esc

Printer-friendly Version

Interactive Discussion



processes are described in Sect. 2.3.2. We only considered the advection effect due to subsurface flows in DOC subsurface 2-dimensional horizontal transport. The DOC carried by subsurface flow will eventually reach a channel system when the water table is higher than the water surface of the channels. The  $q_x$ ,  $q_y$ ,  $q_{sx}$  and  $q_{sy}$  terms in Eqs. (22) and (25) are estimated by solving Eqs. (18) and (21).

## 2.5 Validation

Soil parameters ( $D_s$ ,  $W_s$ ,  $b_{infiltr}$ ) controlling runoff, infiltration and baseflow were adjusted to make the simulated hydrography match the observation at the outlet of our test watershed (see the Sect. 2.6). The comparison was documented in Supplement F. Because DOC concentrations are often measured for large river basins, it is difficult to parameterize the model for specific ecosystem types based on those measurements. Thus, we use the remotely-sensed DOC concentration data to parameterize the DOCDM 1.0. First, following the empirically-based algorithms in Griffin et al. (2011), the river DOC concentrations are estimated by using Landsat5 Thematic Mapper data on 18 July 2003 and 8 May 2004, respectively. Second, we compare our modeled DOC with the satellite-based estimates. Since the DOCDM 1.0 provides DOC channel concentrations on each hour, the model outputs that are closest to the satellite passing time are used for comparison. To spatially compare DOC concentrations from Landsat with the model results, remotely-sensed DOC concentrations are averaged into a 4 km resolution from the original 30 m (Supplement F).

Although the remotely-sensed DOC concentrations are overall higher than those from the simulation, the two datasets have a good relationship (Fig. 4; Supplement F), suggesting that the DOCDM 1.0 can capture the general trend of the watershed-level DOC yield. We are aware of that many parameters in the DOCDM 1.0 may introduce uncertainties and remotely-sensed results are also suffered from cloud contamination, observing angle, and the parameters in their retrieve method. For example, the overestimates in streamflow may be one of the reasons that result in low DOC concentrations in our simulations.

## 2.6 Case study region

To test the DOCDM 1.0, we choose a watershed in the Yukon River Basin as a case study (Fig. 5). The watershed is 6043 km<sup>2</sup> in size and its hydrological unit code (HUC) is 19040505. It is not significantly affected by the exterior stream sources and dominated by boreal forest and shrubland. The rectangle with dark outline in Fig. 5 is the channel network built from the elevation data. Each pixel on the channel has its own depth and width (not shown here). The land cover map is obtained from the University of Maryland's (UMD) 1 km Global Land Cover product (Hansen et al., 2000). Soil parameters (Nijssen et al., 2001a, b) and vegetation parameters including minimum stomatal resistance, albedo, and rooting depth are obtained from the VIC model website (<http://www.hydro.washington.edu/Lettenmaier/Models/VIC/>). The atmosphere forcing data, including precipitation, wind speed, maximum and minimum air temperature, used in the DOCDM 1.0 are acquired from NCEP reanalysis daily data (<http://www.esrl.noaa.gov/psd/data/gridded/data.ncep.reanalysis.surfaceflux.html>). All the input climate data originally have a daily time step and downscaled to an hourly time step using the MT-CLIM model (Kimball et al., 1997; Thornton et al., 1999) for the inputs to our land surface process module that operates on a 1 h time step. We run the DOCDM 1.0 for 1976 and 2004, which are the coldest and warmest years respectively since 1948.

## 3 Results and discussion

### 3.1 Point-level results

The location of our study pixel is denoted as the yellow point in Fig. 5. Its annual average air temperature for 2004 is -4.1 °C, compared to -5.3 °C in 1976. Its average summer (June–August) air temperature is 13.2 and 9.7 °C, respectively (Fig. 6). Its precipitation also shows an upward trend from 499.6 to 775.3 mm yr<sup>-1</sup> during the

# GMDD

8, 10411–10454, 2015

## An integrated Dissolved Organic Carbon Dynamics Model (DOCDM 1.0)

X. Lu and Q. Zhuang

Title Page

Abstract

Introduction

Conclusions

References

Tables

Figures



Back

Close

Full Screen / Esc

Printer-friendly Version

Interactive Discussion







(around 4–7 weeks). After snow melting, rainfall barely resulted in overland events and its DOC concentration is low for the study region.

### 3.3 DOC trend and its environment factors

In the DOCDM 1.0, DOC can leave the watershed from three sources: overland (O), subsurface (S) and soil bottom (B). Water can be further removed by evapotranspiration (ET) in addition to the above three pathways. Water and DOC in overland and subsurface flow first route to channel and then to the river outlet eventually. Water and solute leak from soil bottom will enter the deeper ground layer and may reroute into channel system later. The groundwater in this study refers to both subsurface flow and bottom flow. Here we analyze how water and DOC distribute via those three pathways under changing environment conditions.

We define the annual infiltration ratio as the infiltration to precipitation in a given year. The higher infiltration ratio suggests the more dominant role of the groundwater system. Our simulations showed that the ratio increased from 0.27 to 0.42 during the study period (Fig. 9a). In other words, rainfall and snowmelt water have a larger tendency to join the subsurface, mainly due to increasing air temperature and deepening active layer (Fig. 7). Degrading permafrost increases hydrologic conductivity in soils, facilitating water infiltration.

Despite the increased groundwater, the ratio of overland DOC yield, defined as  $\text{DOC}_O / (\text{DOC}_O + \text{DOC}_S + \text{DOC}_B)$ , yet increased from 0.33 to 0.37 (Fig. 9b). The trend is out of expectation considering the decreasing role of surface transport (Fig. 9a). We believe that increasing soil temperature has two opposite effects on DOC yield. On the one hand, thawing soil makes less surface flow as shown above; on the other hand, increasing DOC production associated with higher soil temperature maintains overland flow as an important component in DOC transport. Although more water leaves the watershed from subsurface flow and bottom flow, relatively low soil temperature and poor organic matter content in deeper soil layers did not result in high DOC production. Therefore, DOC does not follow the recent warming trend. It is necessary to point out

## An integrated Dissolved Organic Carbon Dynamics Model (DOCDM 1.0)

X. Lu and Q. Zhuang

Title Page

Abstract

Introduction

Conclusions

References

Tables

Figures



Back

Close

Full Screen / Esc

Printer-friendly Version

Interactive Discussion





alization here includes the decomposition of both DOC and absorbed DOC. The fact that the absorbed DOC pool has ten times storage of the annual DOC production, suggesting it is necessary to take the sorption and desorption into account. The increasing soil moisture (liquid water) in the thawing months (May–September, not shown here) from 1976 to 2004 reduced DOC production, while the ratio of DOC mineralization to its production changed from 2.32 to 1.64, suggesting that the warming stimulated DOC production in soils. Meanwhile, the ratio of DOC yield to its production also showed a decreasing trend. The thawing soil and the associated hydrological alteration actually slowed down the DOC transport, resulting in more DOC accumulated in soils.

## 4 Conclusions

A catchment-scale DOC model is developed and applied for a watershed in Alaska. DOC flux and concentrations are found to be closely coupled with hydrological dynamics. We find that: (1) the snowmelt period (May–June) dominates the catchment's DOC export, (2) the permafrost thawing and enhancement in groundwater circulation contribute to river discharge in arctic and subarctic basins, (3) permafrost-driven changes in subsurface flow paths and water fluxes influence the flux of DOC from terrestrial to aquatic ecosystems; and (4) Increasing DOC production and more percolation water are two counterbalanced mechanisms in affecting DOC fluxes and concentrations under warming conditions. These dynamics might vary in different watersheds.

There are several limitations in this study. First, the initial condition of the model can induce uncertainty, especially when the simulation period is long. There is no available data as model initial conditions for large temporal scale simulations. Instead, in this study, we first run the VIC model for 10 years to generate an initial state for the DOCDM 1.0. This provides initial conditions for soil moisture and temperature. However, this may not be good way to get initial states for chemical-related variables. For instance, DOC, PDOC1 and PDOC2 are assumed to be zero at the beginning of the simulation. Second, as we have mentioned early, the lower boundary condition for the

### An integrated Dissolved Organic Carbon Dynamics Model (DOCDM 1.0)

X. Lu and Q. Zhuang

Title Page

Abstract

Introduction

Conclusions

References

Tables

Figures



Back

Close

Full Screen / Esc

Printer-friendly Version

Interactive Discussion



water movement equation can significantly affect the hydrological dynamics, in turn, solute simulations. However, a trustable lower boundary condition requires extensive data for various variables. Third, parameters related to DOC production, mineralization, sorption and desorption are uncertain, and might have contributed to simulation uncertainty also. To improve parameterization, verify, and apply the model to the northern high latitudes in quantifying DOC dynamics, more data of DOC and its auxiliary physical, chemical and biological factors for various watersheds will be needed.

## 5 The hardware and software requirements and limitations

DOCDM 1.0 is written in C++ language and can be run in both Microsoft Windows and Linux environments. There is no special requirement for hardware and software to run DOCDM 1.0. All the input data can be readily acquired from internet. The main shortcoming for DOCDM 1.0 is that it is only suitable for relatively small watersheds. Because the lateral water transport is considered in DOCDM 1.0, memory should be allocated to all grid cells at the beginning of simulation, which limits the size of study watershed. In addition, since any given simulation grid cell requires the lateral flow from its neighbor cells, parallel computing is not easily to be implemented.

### Code availability

The code is available under request for academic and non-commercial use. The code is also archived in our lab website (<http://www.eaps.purdue.edu/ebdl/>).

**The Supplement related to this article is available online at doi:10.5194/gmdd-8-10411-2015-supplement.**

## An integrated Dissolved Organic Carbon Dynamics Model (DOCDM 1.0)

X. Lu and Q. Zhuang

Title Page

Abstract

Introduction

Conclusions

References

Tables

Figures

⏪

⏩

◀

▶

Back

Close

Full Screen / Esc

Printer-friendly Version

Interactive Discussion



## An integrated Dissolved Organic Carbon Dynamics Model (DOCDM 1.0)

X. Lu and Q. Zhuang

Title Page

Abstract

Introduction

Conclusions

References

Tables

Figures



Back

Close

Full Screen / Esc

Printer-friendly Version

Interactive Discussion

*Acknowledgements.* This research is supported with projects funded to Q. Zhuang by NSF (DEB-0919331), the NSF Carbon and Water in the Earth Program (NSF-0630319), the NASA Land Use and Land Cover Change program (NASA-NNX09A126G), Department of Energy (DE-FG02-08ER64599), the NSF Division of Information & Intelligent Systems (NSF-1028291), and DOE/Lawrence Berkeley National Laboratory IMPACTS Program. This research was also in part supported by the Director, Office of Science, Office of Biological and Environmental Research of the US Department of Energy under contract no. DE-AC02-05CH11231 as part of their Earth System Modeling Program.

## References

Ågren, A., Haei, M., Köhler, S. J., Bishop, K., and Laudon, H.: Regulation of stream water dissolved organic carbon (DOC) concentrations during snowmelt; the role of discharge, winter climate and memory effects, *Biogeosciences*, 7, 2901–2913, doi:10.5194/bg-7-2901-2010, 2010.

Anderson, E. A.: A Point Energy and Mass Balance Model of a Snow Cover, NOAA Technical Report, US Dept. of Commerce, National Oceanic and Atmospheric Administration, National Weather Service, Office of Hydrology, Silver Spring, MD, 1976.

Andreadis, K. M., Storck, P., and Lettenmaier, D. P.: Modeling snow accumulation and ablation processes in forested environments, *Water. Resour. Res.*, 45, W05429, doi:10.1029/2008WR007042, 2009.

Baker, M., Valett, M., and Dahm, C.: Organic carbon supply and metabolism in a shallow groundwater ecosystem, *Ecology*, 81, 3133–3148, doi:10.2307/177406, 2000.

Bowling, L. C., Pomeroy, J. W., and Lettenmaier, D. P.: Parameterization of blowing-snow sublimation in a macroscale hydrology model, *J. Hydrometeorol.*, 5, 745–762, doi:10.1175/1525-7541(2004)005<0745:POBSIA>2.0.CO;2, 2004.

Boyer, E. B., Hornberger, G. M., Bencala, K. E., and McKnight, D. M.: Overview of a simple model describing variation of dissolved organic carbon in an upland catchment, *Ecol. Model.*, 86, 183–188, doi:10.1016/0304-3800(95)00049-6, 1996.

Boyer, E. B., Hornberger, G. M., Bencala, K. E., and McKnight, D. M.: Effects of asynchronous snowmelt on the flushing of dissolved organic carbon: a mixing model approach,

Hydrol. Process., 18, 3291–3308, doi:10.1002/1099-1085(20001230)14:18<3291::AID-HYP202>3.0.CO;2-2, 2000.

Celia, M. A., Bouloutas, E. T., and Zarba, R. L.: A general mass-conservative numerical solution for the unsaturated flow equation, *Water. Resour. Res.*, 26, 1483–1496, doi:10.1029/WR026i007p01483, 1990.

Cherkauer, K. A. and Lettenmaier, D. P.: Hydrologic effects of frozen soils in the upper Mississippi River Basin, *J. Geophys. Res.*, 104, 19599–19610, doi:10.1029/1999JD900337, 1999.

Cherkauer, K. A. and Lettenmaier, D. P.: Simulation of spatial variability in snow and frozen soil, *J. Geophys. Res.*, 108, 8858, doi:10.1029/2003JD003575, 2003.

Cherkauer, K. A., Bowling, L. C., and Lettenmaier, D. P.: Variable infiltration capacity cold land process model updates, *Global Planet. Change*, 38, 151–159, doi:10.1016/S0921-8181(03)00025-0, 2003.

Dickinson, R. E., Henderson-Sellers, A., Kennedy, P. J., and Wilson, M. F.: Biosphere–Atmosphere Transfer Scheme (BATS) for the NCAR Community Climate Model, NCAR Tech. Note TN-275+STR, National Center For Atmospheric Research, Boulder, CO, 1986.

Dittmar, T. and Kattner, G.: The biogeochemistry of the river and shelf ecosystem of the Arctic Ocean: a review, *Mar. Chem.*, 83, 103–120, doi:10.1016/S0304-4203(03)00105-1, 2003.

Dutta, K., Schuur, E. A. G., Neff, J. C., and Zimov, S. A.: Potential carbon release from permafrost soils of northeastern Siberia, *Global Change. Biol.*, 12, 2336–2351, doi:10.1111/j.1365-2486.2006.01259.x, 2006.

Fan, Z., Neff, J. C., and Wickland, K. P.: Modeling the production, decomposition, and transport of dissolved organic carbon in Boreal soils, *Soil Sci.*, 175, 223–232, doi:10.1097/SS.0b013e3181e0559a, 2010.

Flerchinger, G. N. and Saxton, K. E.: Simultaneous heat and water model of a freezing snow-residue-soil system, I. Theory and development, *T. ASAE*, 32, 565–571, doi:10.13031/2013.31040, 1989.

Freeman, C., Evans, C. D., Monteith, D. T., Reynolds, B., and Fenner, N.: Export of organic carbon from peat soils, *Nature*, 412, 785, doi:10.1038/35090628, 2001.

Futter, M. N., Butterfield, D., Cosby, B. J., Dillon, P. J., Wade, A. J., and Whitehead, P. G.: Modeling the mechanisms that control in-stream dissolved organic carbon dynamics in upland and forested catchments, *Water. Resour. Res.*, 43, W02424, doi:10.1029/2006WR004960, 2007.

## GMDD

8, 10411–10454, 2015

### An integrated Dissolved Organic Carbon Dynamics Model (DOCDM 1.0)

X. Lu and Q. Zhuang

Title Page

Abstract

Introduction

Conclusions

References

Tables

Figures

⏪

⏩

◀

▶

Back

Close

Full Screen / Esc

Printer-friendly Version

Interactive Discussion



## An integrated Dissolved Organic Carbon Dynamics Model (DOCDM 1.0)

X. Lu and Q. Zhuang

Title Page

Abstract

Introduction

Conclusions

References

Tables

Figures

◀

▶

◀

▶

Back

Close

Full Screen / Esc

Printer-friendly Version

Interactive Discussion



- Gorham, E.: Northern peatlands: role in the carbon cycle and probable responses to climatic warming, *Ecol. Econ.*, 1, 182–195, doi:10.2307/1941811, 1991.
- Griffin, C. G., Frey, K. E., Rogan, J., and Holmes, R. M.: Spatial and interannual variability of dissolved organic matter in the Kolyma River, east Siberia, observed using satellite imagery, *J. Geophys. Res.*, 116, G03018, doi:10.1029/2010JG001634, 2011.
- Hansen, M. C., DeFries, R. S., Townshend, J. R. G., and Sohlberg, R.: Global land covers classification at 1 km resolution using a classification tree approach, *Int. J. Remote. Sens.*, 21, 1331–1364, doi:10.1080/014311600210209, 2000.
- Hansson, K., Šimůnek, J., Mizoguchi, M., and Lundin, L. C.: Water flow and heat transport in frozen soil: numerical solution and freeze/thaw applications, *Vadose Zone J.*, 3, 693–704, doi:10.2113/3.2.693, 2004.
- Hinzman, L. D., Bettez, N. D., Bolton, W. R., Chapin, F. S., Dyurgerov, M. B., Fastie, C. L., Griffith, B., Hollister, R. D., Hope, A., Huntington, H. P., Jensen, A. M., Jia, G. J., Jorgenson, T., Kane, D. L., Klein, D. R., Kofinas, G., Lynch, A. H., Lloyd, A. H., McGuire, A. D., Nelson, F. E., Oechel, W. C., Osterkamp, T. E., Racine, C. H., Romanovsky, V. E., Stone, R. S., Stow, D. A., Sturm, M., Tweedie, C. E., Vourlitis, G. L., Walker, M. D., Walker, D. A., Webber, P. J., Welker, J. M., Winker, K. S., and Yoshikawa, K.: Evidence and implications of recent climate change in northern Alaska and other arctic regions, *Climatic Change*, 72, 251–298, doi:10.1007/s10584-005-5352-2, 2005.
- Holmes, R. M., McClell, J. W., Raymond, P. A., Frazer, B. B., Peterson, B. J., and Stieglitz, M.: Lability of DOC transported by Alaskan rivers to the arctic ocean, *Geophys. Res. Lett.*, 35, L03402, doi:10.1029/2007GL032837, 2008.
- Hornberger, G. M., Bencala, K. E., and McKnight, D. M.: Hydrological controls on the temporal variation of dissolved organic carbon in the Snake River near Montezuma, Colorado, *Biogeochemistry*, 25, 147–165, doi:10.1007/BF00024390, 1994.
- Johansen, O.: Thermal Conductivity of Soils, PhD thesis, Institute for Kjøleteknik, Trondheim, Norway, 1975.
- Julien, P. Y. and Saghafian, B.: CASC2D User's Manual – A Two Dimensional Watershed Rainfall-Runoff Model, Colorado State University, Fort Collins, Fort Collins, CO, 1991.
- Julien, P. Y., Saghafian, B., and Ogden, F. L.: Raster-based hydrologic modeling of spatially-varied surface runoff, *Water Resour. Bull.*, 31, 523–536, doi:10.1111/j.1752-1688.1995.tb04039.x, 1995.

## An integrated Dissolved Organic Carbon Dynamics Model (DOCDM 1.0)

X. Lu and Q. Zhuang

Title Page

Abstract

Introduction

Conclusions

References

Tables

Figures



Back

Close

Full Screen / Esc

Printer-friendly Version

Interactive Discussion



Kalbitz, K., Schwesig, D., Retnemeyer, J., and Matzer, E.: Stabilization of the dissolved organic matter by sorption to the mineral soil, *Soil Biol. Biochem.*, 37, 1319–1331, doi:10.1016/j.soilbio.2004.11.028, 2005.

Karlstrom, H.: Peat Characteristics: Based on Multivariate Data Analysis of Magnetic Resonance Spectroscopy Data, Umea Univ., Umea, Sweden, 1995.

Kimball, J. S., Running, S. W., and Nemani, R.: An improved method for estimating surface humidity from daily minimum temperature, *Agr. Forest Meteorol.*, 85, 87–98, doi:10.1016/S0168-1923(96)02366-0, 1997.

Liang, X., Lettenmaier, D. P., Wood, E. F., and Burges, S. J.: A simple hydrologically based model of land-surface water and energy fluxes for general-circulation models, *J. Geophys. Res.*, 99, 14415–14428, doi:10.1029/94JD00483, 1994.

Lobbess, J. M., Fitznar, H. P., and Kattner, G.: Biogeochemical characteristics of dissolved and particulate organic matter in Russian rivers entering the Arctic Ocean, *Geochim. Cosmochim. Acta*, 64, 2973–2983, doi:10.1016/S0016-7037(00)00409-9, 2000.

Lu, X. L. and Zhuang, Q.: Areal changes of land ecosystems in the Alaskan Yukon River Basin from 1984 to 2008, *Environ. Res. Lett.*, 6, 034012, doi:10.1088/1748-9326/6/3/034012, 2011.

Lundin, L. C.: Hydraulic properties in an operational model of frozen soil, *J. Hydrol.*, 118, 289–310, doi:10.1016/0022-1694(90)90264-X, 1990.

Mei, Y., Hornberger, G. M., Kaplan, L. A., Denis, N. J., and Aufdenkampe, A. K.: Estimation of dissolved organic carbon contribution from hillslope soils to a headwater stream, *Water Resour. Res.*, 48, W09514, doi:10.1029/2011WR010815, 2012.

Michalzik, B. and Matzner, E.: Dynamics of dissolved organic nitrogen and carbon in a Central European Norway spruce ecosystem, *Eur. J. Soil Sci.*, 50, 579–590, doi:10.1046/j.1365-2389.1999.00267.x, 1999.

Michalzik, B., Tipping, E., Mulder, J., Gallardo, L. J. F., Matzner, E., Bryant, C. L., Clarke, N., Lofts, S., and Vicente Esteban, M. A.: Modeling the production and transport of dissolved organic carbon in forest soils, *Biogeochemistry*, 66, 241–264, doi:10.1023/B:BI0G.0000005329.68861.27, 2003.

Monteith, J. L. and Unsworth, M. H.: Principles of Environmental Physics, 2nd edn., Routledge, Chapman and Hall, New York, 1990.

Moore, P. D.: The future of cool temperate bogs, *Environ. Conserv.*, 29, 3–20, doi:10.1017/S0376892902000024, 2002.

## An integrated Dissolved Organic Carbon Dynamics Model (DOCDM 1.0)

X. Lu and Q. Zhuang

Title Page

Abstract

Introduction

Conclusions

References

Tables

Figures

◀

▶

◀

▶

Back

Close

Full Screen / Esc

Printer-friendly Version

Interactive Discussion



Moore, T. R., Roulet, N. T., and Waddington, J. M.: Uncertainties in predicting the effect of climatic change on the carbon cycling of Canadian peatlands, *Climatic Change*, 40, 229–245, doi:10.1023/A:1005408719297, 1998.

Morris, D. P. and Hargreaves, B. R.: The role of photochemical degradation of dissolved organic carbon in regulating the UV transparency of 3 lakes on the Pocono Plateau, *Limnol. Oceanogr.*, 42, 239–249, 1997.

Neff, J. C. and Asner, G. P.: Dissolved organic carbon in terrestrial ecosystems: synthesis and a model, *Ecosystems*, 4, 29–48, doi:10.1007/s100210000058, 2001.

Nijssen, B., O'Donnell, G. M., Hamlet, A. F., and Lettenmaier, D. P.: Hydrologic sensitivity of global rivers to climate change, *Climatic Change*, 50, 143–175, doi:10.1023/A:1010616428763, 2001a.

Nijssen, B., O'Donnell, G. M., Lettenmaier, D. P., Lohmann, D., and Wood, E. F.: Predicting the discharge of global rivers, *J. Climate*, 14, 3307–3323, doi:10.1175/1520-0442(2001)014<3307:PTDOGR>2.0.CO;2, 2001b.

Patankar, S. V.: *Numerical Heat Transfer and Fluid Flow*, Computational Methods in Mechanics and Thermal Science Series, Hemisphere, New York, 1980.

Qualls, R. G. and Haines, B. L.: Geochemistry of dissolved organic nutrients in water percolating through a forest ecosystem, *Soil Sci. Soc. Am. J.*, 55, 1112–1123, 1991.

Qualls, R. G. and Haines, B. L.: Biodegradability of dissolved organic matter in forest throughfall, soil solution, and stream water, *Soil Sci. Soc. Am. J.*, 56, 578–586, 1992a.

Qualls, R. G. and Haines, B. L.: Measuring adsorption isotherms using continuous, unsaturated flow through intact soil cores, *Soil Sci. Soc. Am. J.*, 56, 456–460, 1992b.

Raymond, P. A. and Bauer, J. E.: Bacterial consumption of DOC during transport through a temperate estuary, *Aquat. Microb. Ecol.*, 22, 1–12, doi:10.3354/ame022001, 2000.

Raymond, P. A., McClelland, J. W., Holmes, R. M., Zhulidov, A. V., Mull, K., Peterson, B. J., Striegl, R. G., Aiken, G. R., and Gurtovaya, T. Y.: Flux and age of dissolved organic carbon exported to the Arctic Ocean: a carbon isotopic study of the five largest arctic rivers, *Global Biogeochem. Cy.*, 21, GB4011, doi:10.1029/2007GB002934, 2007.

Reeve, A. S., Siegel, D. I., and Glaser, P. H.: Simulating vertical flow in large peatlands, *J. Hydrol.*, 227, 207–217, doi:10.1016/S0022-1694(99)00183-3, 2001.

Richards, L. A.: Capillary conduction of liquids through porous mediums, *Physics*, 1, 318–333, 1931.



Woolhiser, D. A.: Simulation of unsteady overland flow, in: Unsteady Flow in Open Channels, edited by: Mahmood, K. and Yevjevich, V., Fort Collins, Colorado, 485–508, 1975.

Xu, N. and Saiers, J. E.: Temperature and hydrologic controls on dissolved organic matter mobilization and transport within a forest topsoil, Environ. Sci. Technol., 44, 5423–5429, doi:10.1021/es1002296, 2010.

Yurova, A., Sirin, A., Buffam, I., Bishop, K., and Laudon, H.: Modeling the dissolved organic carbon output from a boreal mire using the convection-dispersion equation: importance of representing sorption, Water. Resour. Res., 44, W07411, doi:10.1029/2007WR006523, 2008.

Zhang, X. C., Norton, C. D., and Nearing, M. A.: Chemical transfer from soil solution to surface runoff, Water. Resour. Res., 33, 809–815, doi:10.1029/96WR03908, 1997.

## GMDD

8, 10411–10454, 2015

### An integrated Dissolved Organic Carbon Dynamics Model (DOCDM 1.0)

X. Lu and Q. Zhuang

Title Page

Abstract

Introduction

Conclusions

References

Tables

Figures

⏪

⏩

◀

▶

Back

Close

Full Screen / Esc

Printer-friendly Version

Interactive Discussion





## An integrated Dissolved Organic Carbon Dynamics Model (DOCDM 1.0)

X. Lu and Q. Zhuang

Title Page

Abstract

Introduction

Conclusions

References

Tables

Figures



Back

Close

Full Screen / Esc

Printer-friendly Version

Interactive Discussion



**Table 2.** The ratios of DOC production to its sorption, mineralization and transport in 1976 and 2004.

Ratios	1976	2004
$\frac{\text{DOC}_{\text{production}}}{\text{DOC}_{\text{sorption}}}$	8.68 %	5.25 %
$\frac{\text{DOC}_{\text{production}}}{\text{DOC}_{\text{mineralization}}}$	42.92 %	60.95 %
$\frac{\text{DOC}_{\text{production}}}{\text{DOC}_{\text{transport}}}$	74.45 %	161.50 %

## An integrated Dissolved Organic Carbon Dynamics Model (DOCDM 1.0)

X. Lu and Q. Zhuang

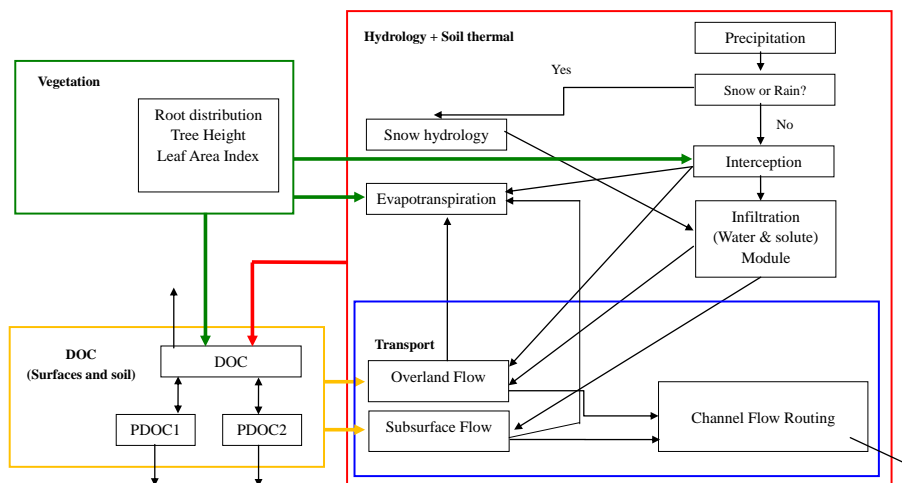


**Figure 1.** DOCDM 1.0 framework of hydrology, vegetation and DOC dynamics. See Supplement A for more details of description. The processes of DOC dynamics (yellow part) are further illustrated in Fig. 2.

## An integrated Dissolved Organic Carbon Dynamics Model (DOCDM 1.0)

X. Lu and Q. Zhuang

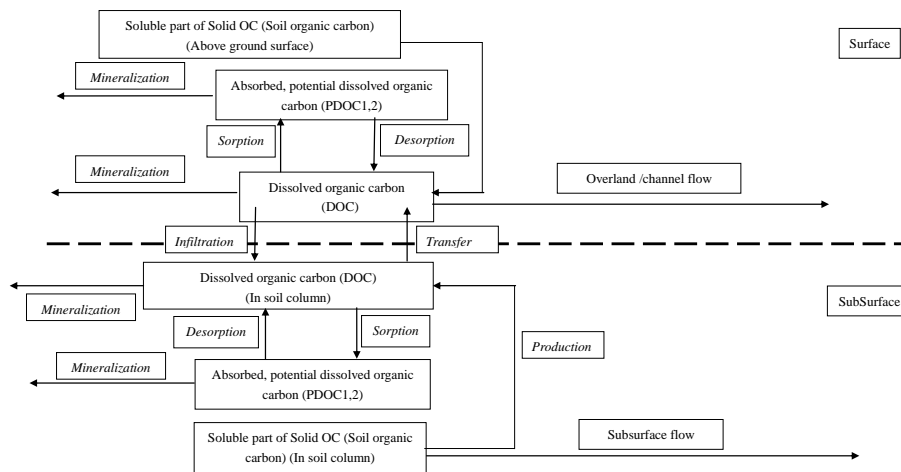


**Figure 2.** Schematic diagram of the pools of soluble organic matter (DOC and PDOC) and production, mineralization and adsorption and desorption processes (the yellow part in Fig. 1).

Title Page

Abstract

Introduction

Conclusions

References

Tables

Figures



Back

Close

Full Screen / Esc

Printer-friendly Version

Interactive Discussion



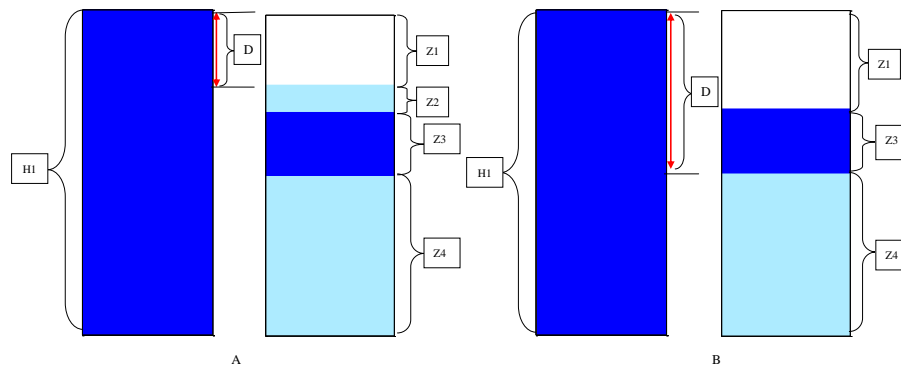
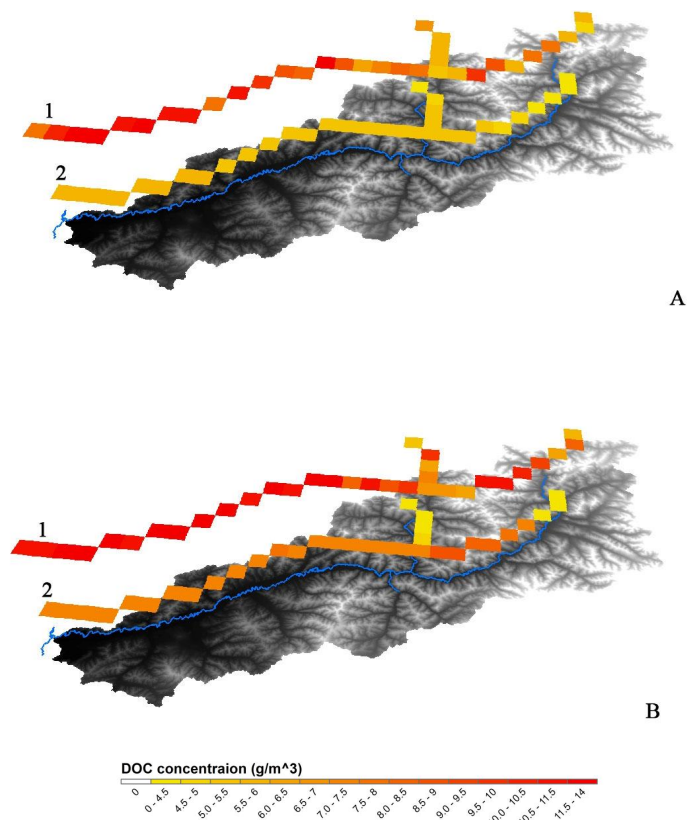


**Figure 3.** The two scenarios for the saturated subsurface flow between adjacent neighbors. Grey, blue and white represent ice, liquid saturated and unsaturated regions in soil column, respectively. H1: saturated layer in soil column. Z1: possible top unsaturated layer. Z2: possible ice layer. Z3: possible liquid saturated layer. Z4: possible bottom ice layer.  $D$ : effective aquifer thickness.

[Title Page](#)
[Abstract](#)
[Introduction](#)
[Conclusions](#)
[References](#)
[Tables](#)
[Figures](#)
[⏪](#)
[⏩](#)
[◀](#)
[▶](#)
[Back](#)
[Close](#)
[Full Screen / Esc](#)
[Printer-friendly Version](#)
[Interactive Discussion](#)

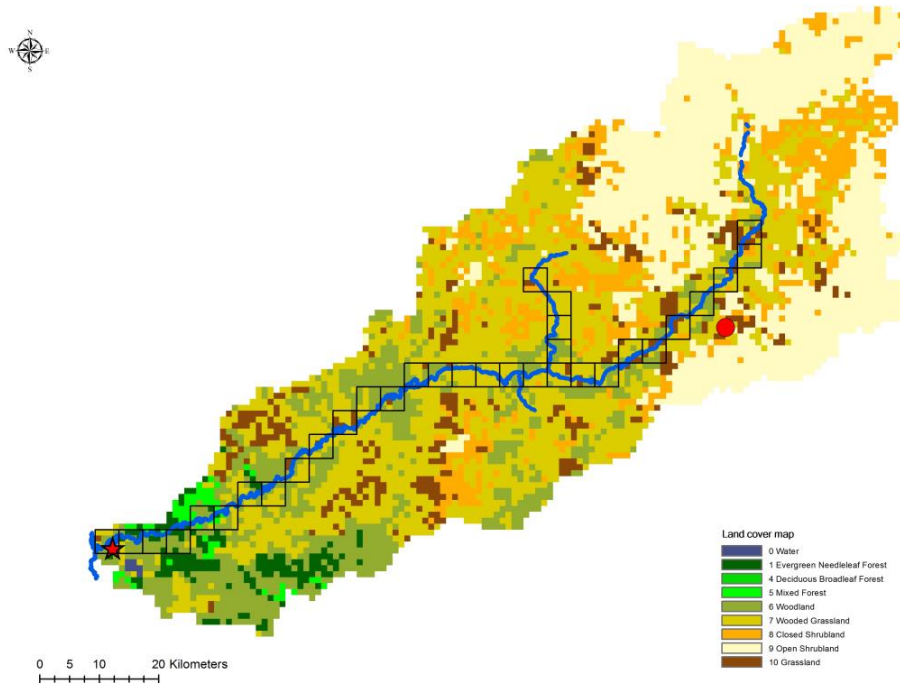

## An integrated Dissolved Organic Carbon Dynamics Model (DOCDM 1.0)

X. Lu and Q. Zhuang



**Figure 4.** The DOC validation results for days of 18 July 2003 **(a)** and 5 August 2004 **(b)**. Numbers 1 and 2 stand for the satellite observation and simulations, respectively. The river network and elevation are also displayed as background.

[Title Page](#)
[Abstract](#)
[Introduction](#)
[Conclusions](#)
[References](#)
[Tables](#)
[Figures](#)
[◀](#)
[▶](#)
[◀](#)
[▶](#)
[Back](#)
[Close](#)
[Full Screen / Esc](#)
[Printer-friendly Version](#)
[Interactive Discussion](#)

**Figure 5.** The land cover map for the test watershed (HUC 19040405). The red star stands for the river outlet and the red solid circle is the demonstration point. The resolution for this map is 1 km. The simulation grids (4 km in this study) with dark outline have the river channel in them.

**An integrated  
Dissolved Organic  
Carbon Dynamics  
Model (DOCDM 1.0)**

X. Lu and Q. Zhuang

Title Page

Abstract

Introduction

Conclusions

References

Tables

Figures

⏪

⏩

◀

▶

Back

Close

Full Screen / Esc

Printer-friendly Version

Interactive Discussion



## An integrated Dissolved Organic Carbon Dynamics Model (DOCDM 1.0)

X. Lu and Q. Zhuang

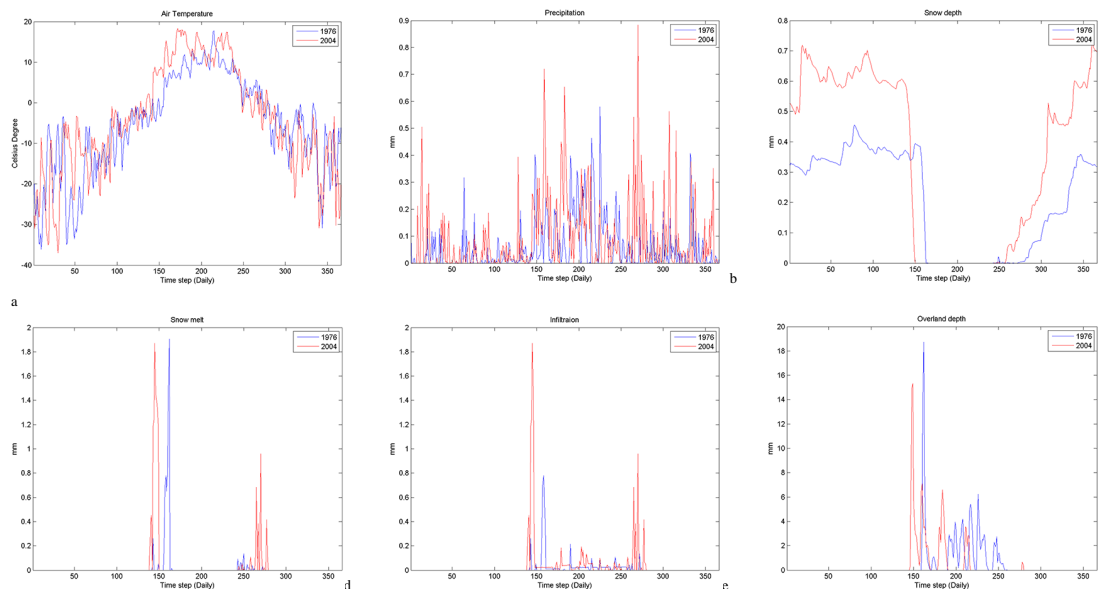


**Figure 6.** The model outputs on the demonstraion point in 1976 and 2004: **(a)** air temperaure **(b)** precipitatin **(c)** snow depth **(d)** snowmelt **(e)** infiltration and **(f)** overland depth.

## An integrated Dissolved Organic Carbon Dynamics Model (DOCDM 1.0)

X. Lu and Q. Zhuang

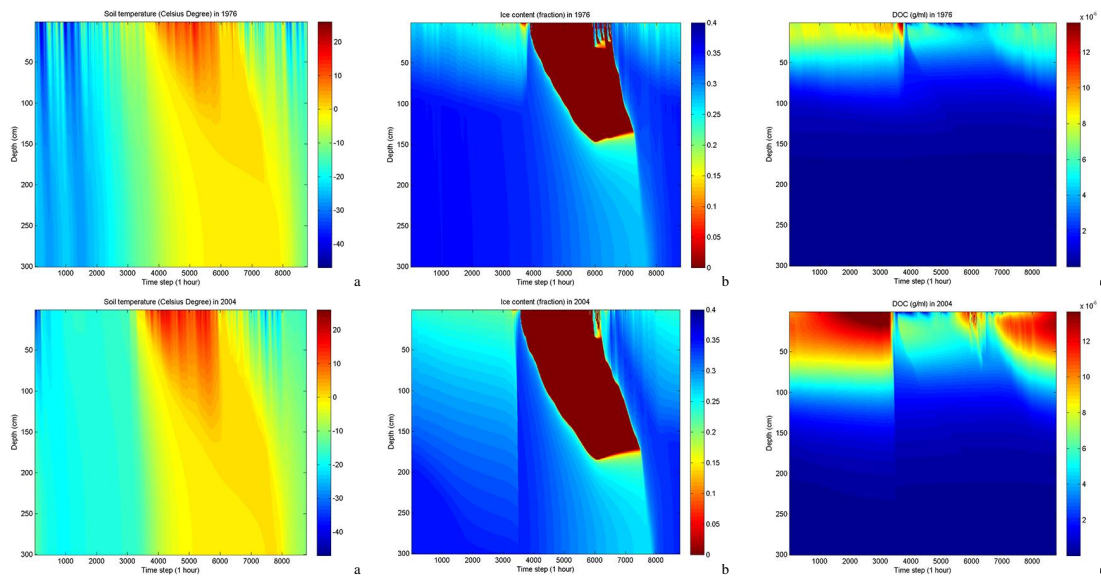


**Figure 7.** The model outputs in 1976 and 2004: **(a)** soil temperature **(b)** ice content and **(c)** DOC concentration profile. The time step is one hour.

Title Page

Abstract

Introduction

Conclusions

References

Tables

Figures



Back

Close

Full Screen / Esc

Printer-friendly Version

Interactive Discussion





## An integrated Dissolved Organic Carbon Dynamics Model (DOCDM 1.0)

X. Lu and Q. Zhuang

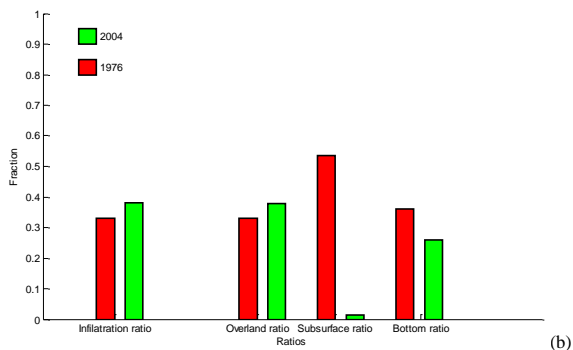
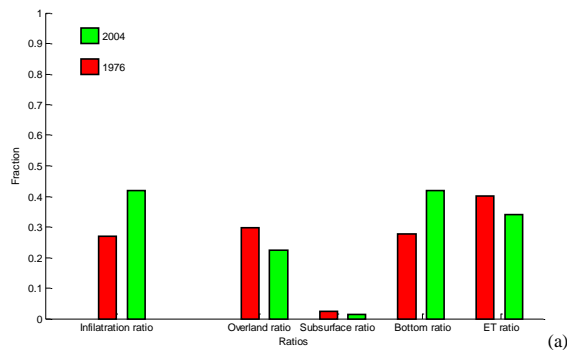


**Figure 9.** The change of water **(a)** and DOC **(b)** infiltration ratio and their transport pathways in 1976 and 2004.

Title Page

Abstract Introduction

Conclusions References

Tables Figures

◀ ▶

◀ ▶

Back Close

Full Screen / Esc

Printer-friendly Version

Interactive Discussion

